Supplementary Figure 1

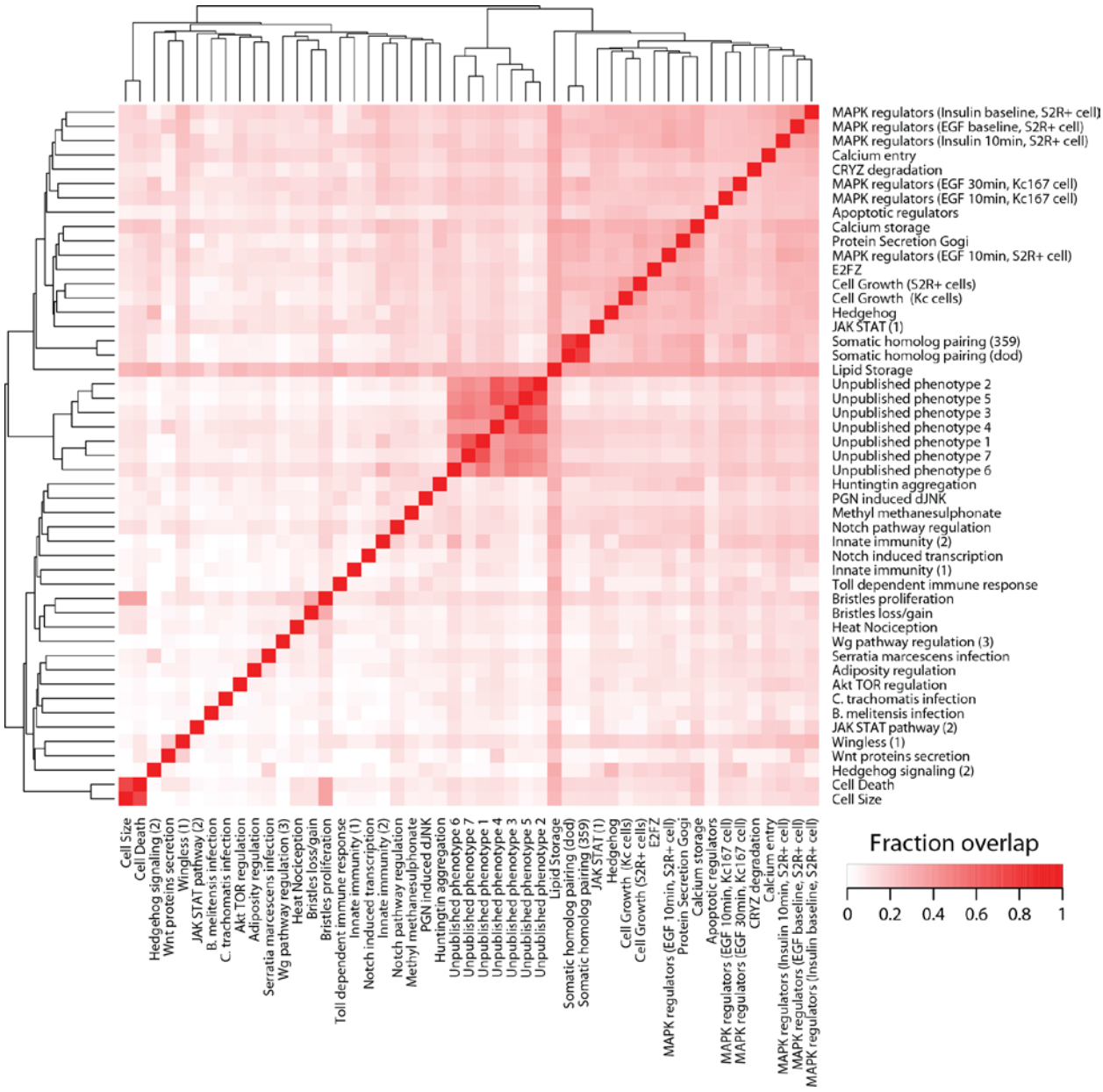

Supplementary Figure 1: Relationship between 49 RNAi screens. The heat map shows the fraction of hits overlapping between the screens. Average overlap between screens is 14%**.**

Nature Methods: doi:10.1038/nmeth.2733

Supplementary Figure 2

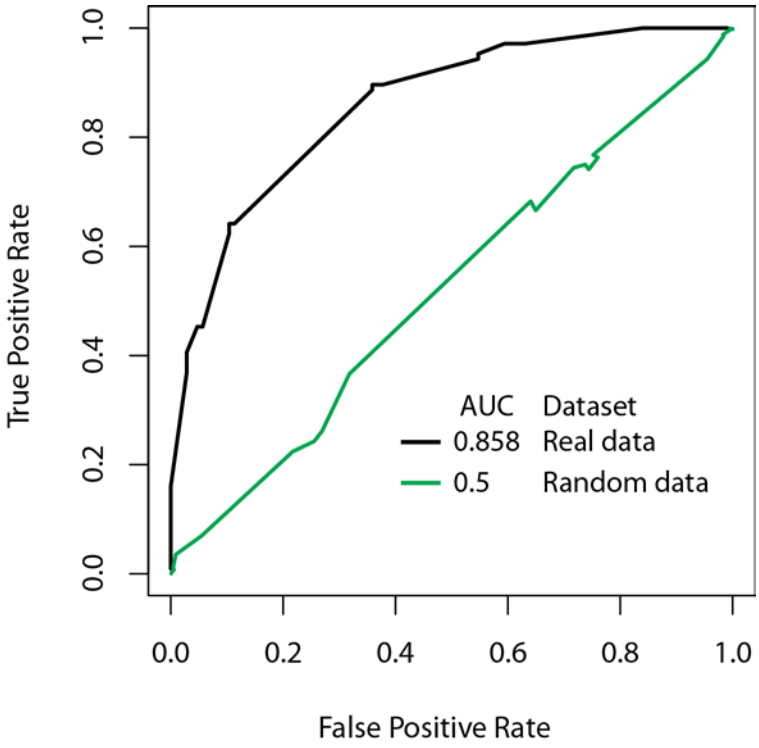

Supplementary Figure 2: ROC plots comparing performance of sign score against random and real phenotype matrix (RNAi signatures). The predictive performance of sign score is compared with real and random data. The random data refers to randomized phenotype matrix, where the signatures are preserved but the genes IDs are randomly permuted. The TPR and FPR values are computed at various sign score cutoff values for both the real and random dataset. In the ROC plot the green and black line corresponds to random and real dataset set respectively. Note that the green line is an average of 100 random datasets.

Nature Methods: doi:10.1038/nmeth.2733

Supplementary Figure 3

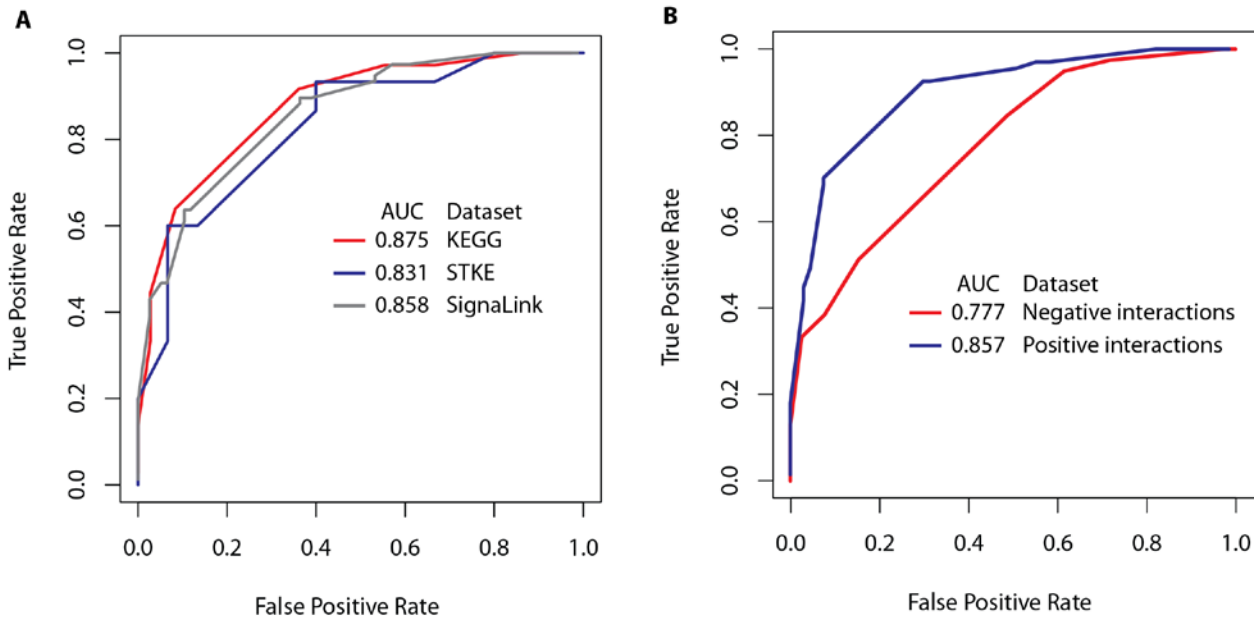

Supplementary Figure 3: ROC plots comparing the subset of reference interactions and comparing performance of positive and negative interactions. A) ROC plot corresponding to the performance of reference set derived from different signaling pathways (number of interactions in KEGG is 36, STKE is 15 and SignaLink is 77). Figure shows that the sign prediction model has similar predictive power for reference sets derived from different signaling pathway databases. B) ROC plot corresponding to the positive and negative edge sign predictions. The blue line corresponds to performance of positive interactions and red line corresponds to negative interactions (number of positive interactions are 67 and a negative interactions are 39).

Nature Methods: doi:10.1038/nmeth.2733

Supplementary Figure 4

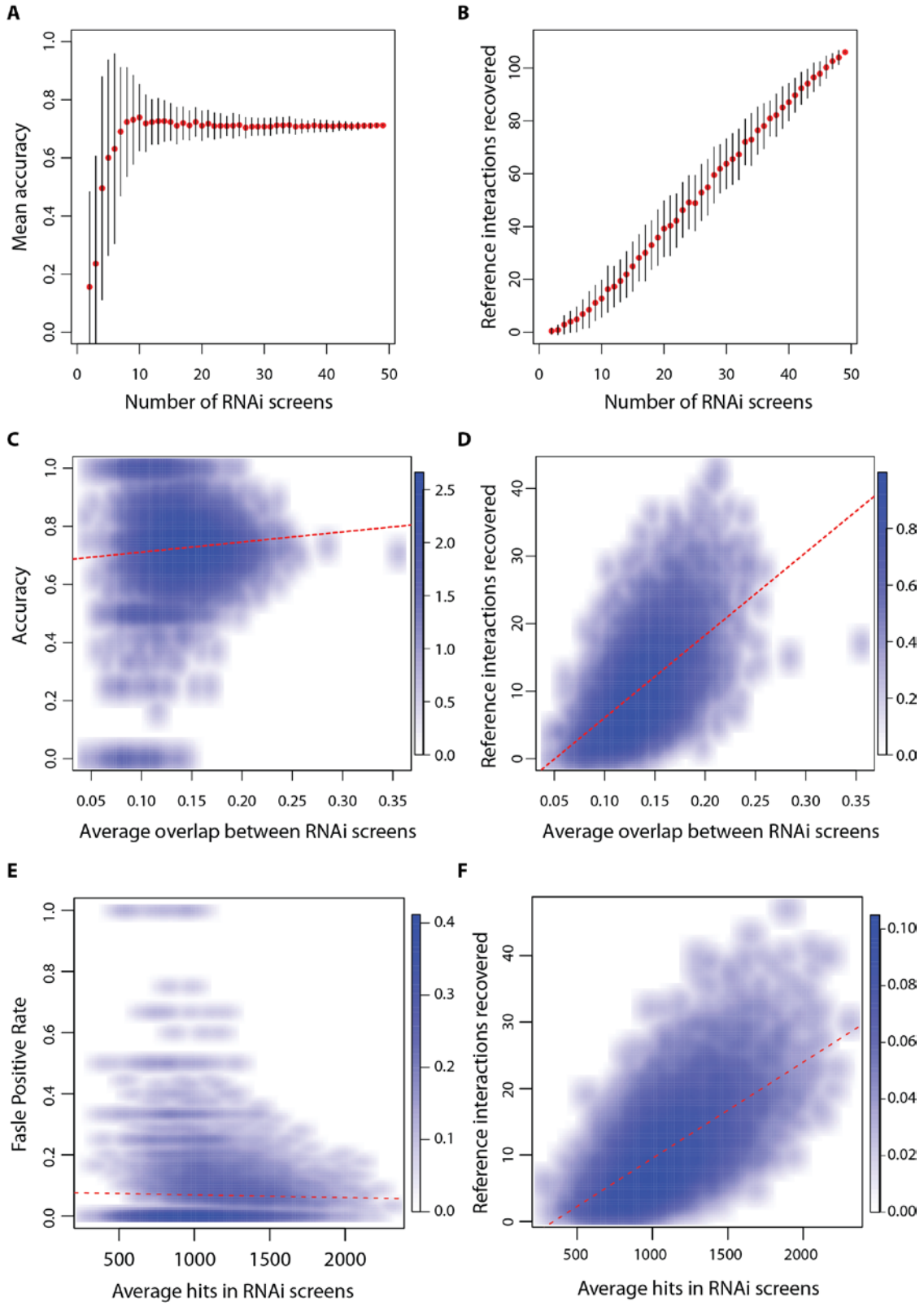

Nature Methods: doi:10.1038/nmeth.2733

Supplementary Figure 4: continued

Supplementary Figure 4: Robustness of sign score prediction performance.

A) Estimated the accuracy of the sign prediction models with various number RNAi screens ranging from minimum of 2 screens to maximum of 49 screens. The accuracy value shows the proportion of true predictions from total prediction and it is computed as accuracy = (TP + TN) / (TP + FP + FN + TN). For each screen cutoff value, 100 random subsets were sampled and the mean and standard deviation of the accuracy value was computed. The plot shows mean accuracy value against the number of screens. Note the accuracy is computed at sign score cutoff of ≥ 1 or ≤ -1.

B) Analysis same as above (A). For each screen cutoff average number of reference interaction recovered and standard deviation is computed and plotted.

C) Density scatter plot showing the lack of correlation between the accuracy and the similarity between the RNAi screens (Pearson's correlation = 0.07). 9 RNAi screens are randomly sampled and the average overlap between the screens and accuracy values at sign score cutoff ≥ 1 or ≤ -1 was computed. Repeated this random sampling 10,000 times and plotted the accuracy against average overlap between the screens. The red dotted line is regression line showing no correlation.

D) Analysis same as above (C). Number of reference interaction recovered is plotted against average overlap between the screens. The red dotted line is regression line showing positive correlation (Pearson's correlation = 0.56).

E) Density scatter plot showing the lack of correlation between accuracy and average hit frequency in RNAi screens. 9 RNAi screens are randomly sampled and the average hit frequency and accuracy values at sign score cutoff ≥ 1 or ≤ -1 was computed. Repeated this random sampling 10,000 times and plotted the accuracy vs. RNAi hit frequency. The red dotted line is regression line showing no correlation.

F) Analysis same as above (E). Number of reference interaction recovered is plotted against average hit frequency in RNAi screens. The red dotted line is regression line showing positive correlation.

Nature Methods: doi:10.1038/nmeth.2733

Supplementary Figure 5

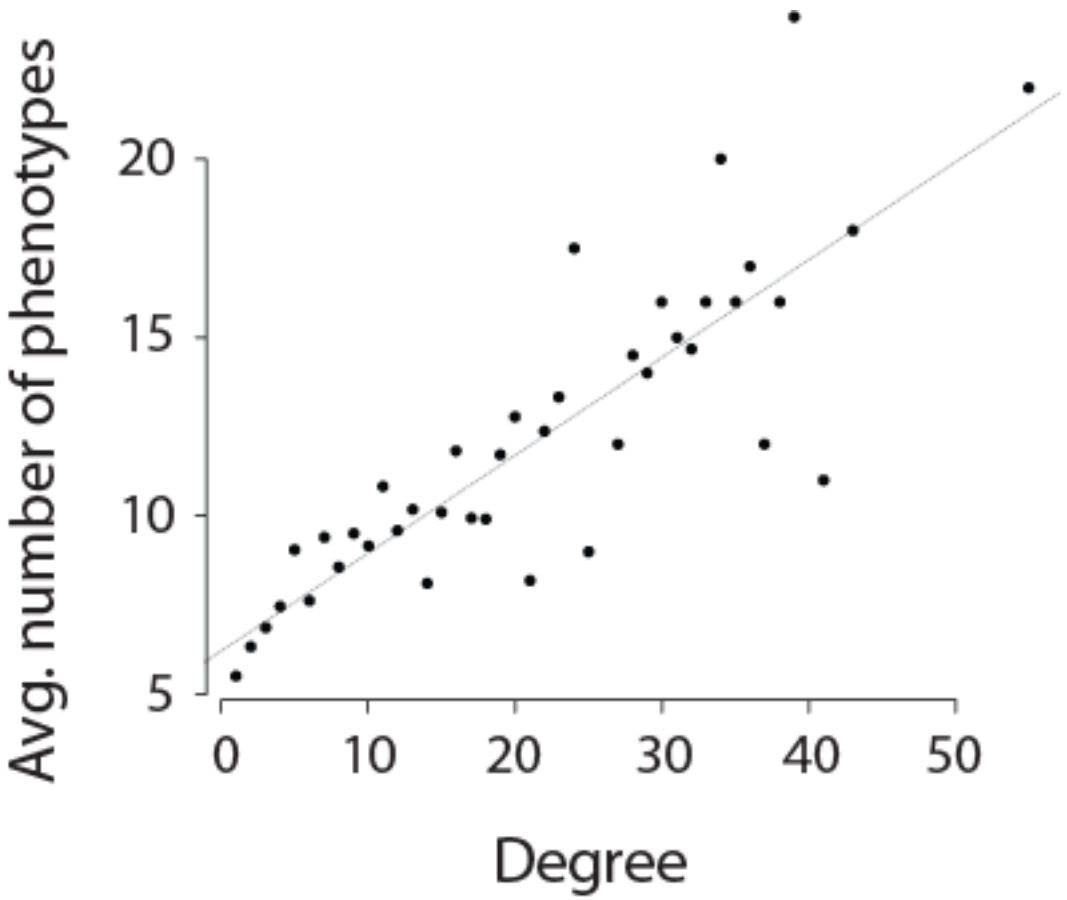

Supplementary Figure 5: Correlation between the node degree (number of neighbors) and the number of phenotypes a gene regulates. The positive correlation could be due to the fact that a gene regulating multiple phenotypes has a higher chance of scoring with other interacting proteins.

Nature Methods: doi:10.1038/nmeth.2733

Supplementary Figure 6

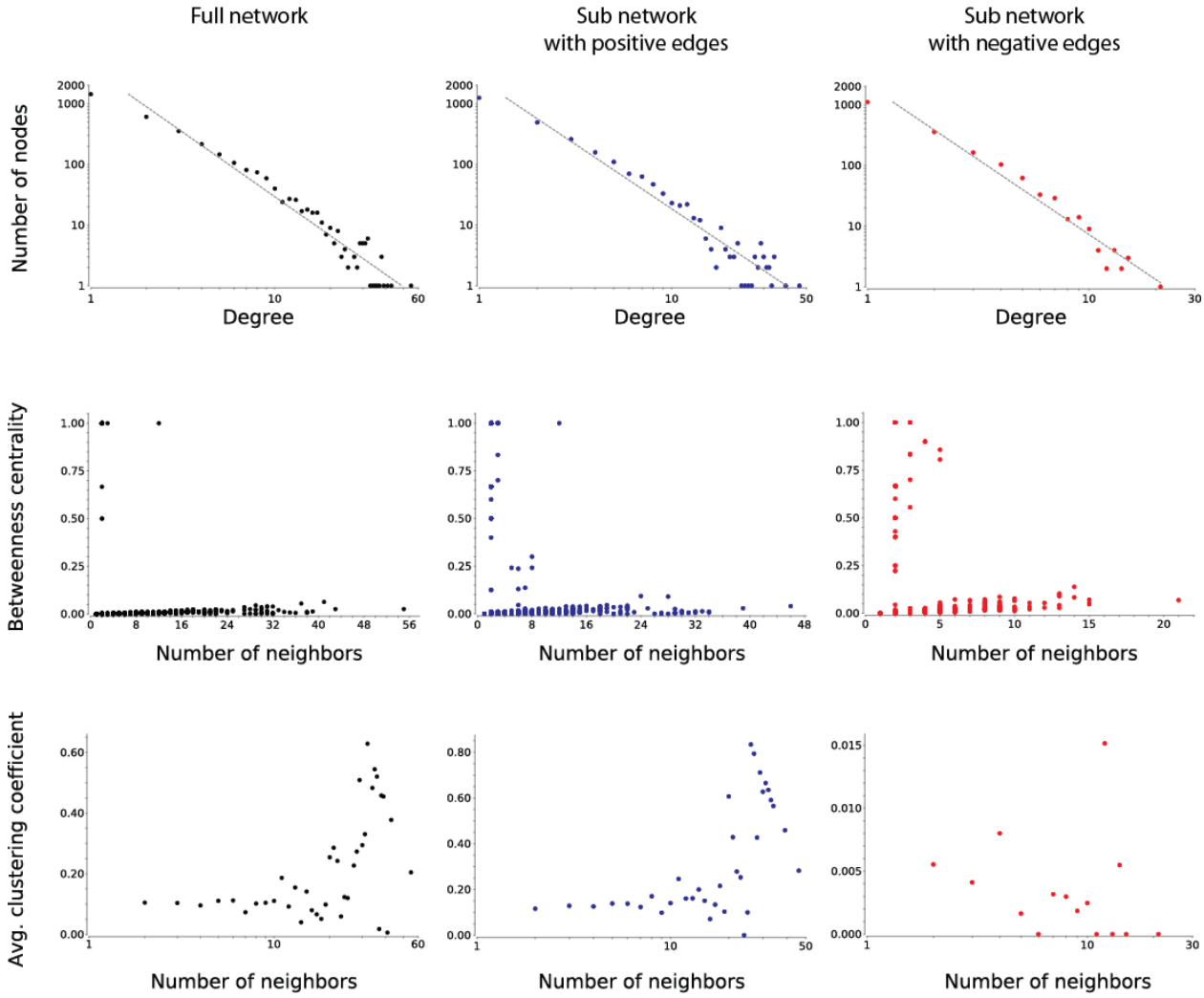

Supplementary Figure 6: Network properties of the signed network. The full network and sub-networks with positive or negative interactions show similar degree distribution, and node betweenness centrality. However, clustering coefficient vs. number of neighbors shows striking difference between positive and negative edges.

Nature Methods: doi:10.1038/nmeth.2733

Supplementary Figure 7

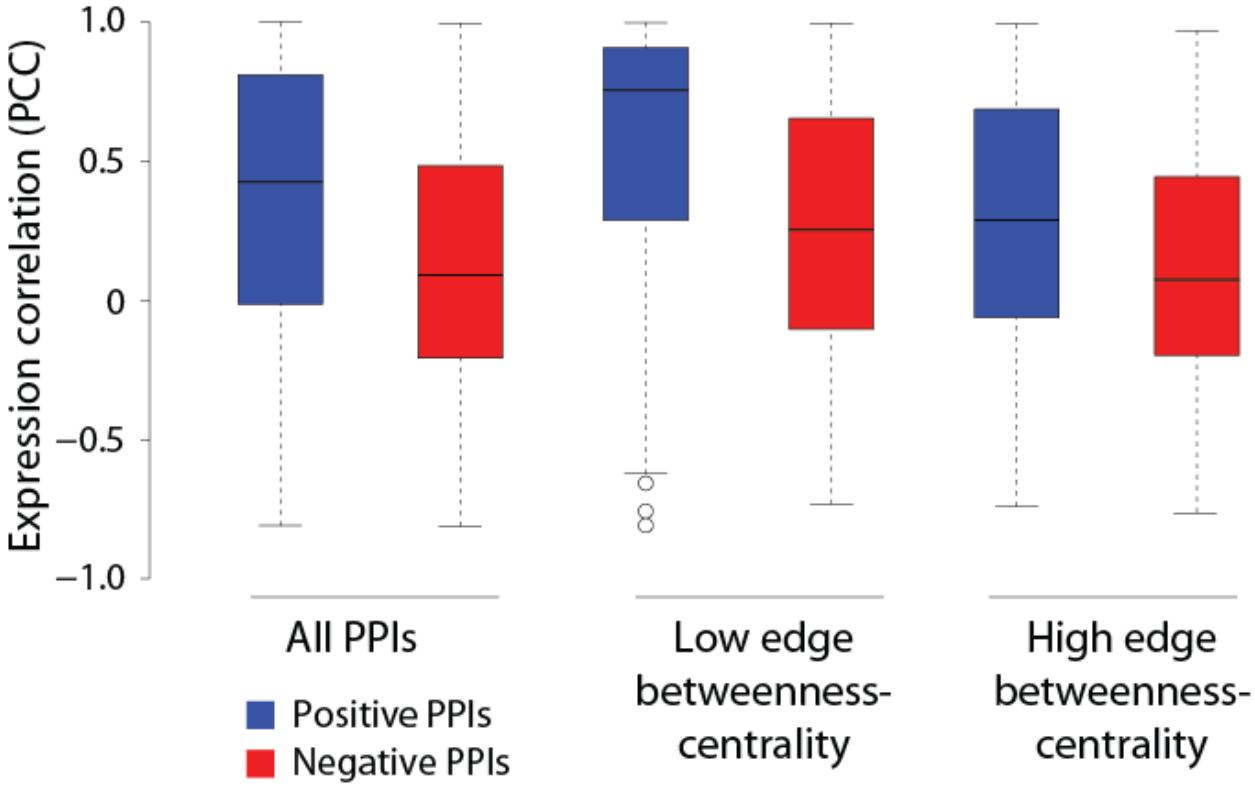

Supplementary Figure 7: Correlation of edge signs and gene expression correlation. We observe significant differences in expression correlation with respect to edge betweenness-centrality. Both positive and negative interactions with low edge betweenness-centrality tend to shows positive PCC than high edge betweenness-centrality (p-value 2.2e-6 and 6.635e-05 respectively; Wilcox test).

Nature Methods: doi:10.1038/nmeth.2733

Supplementary Figure 8

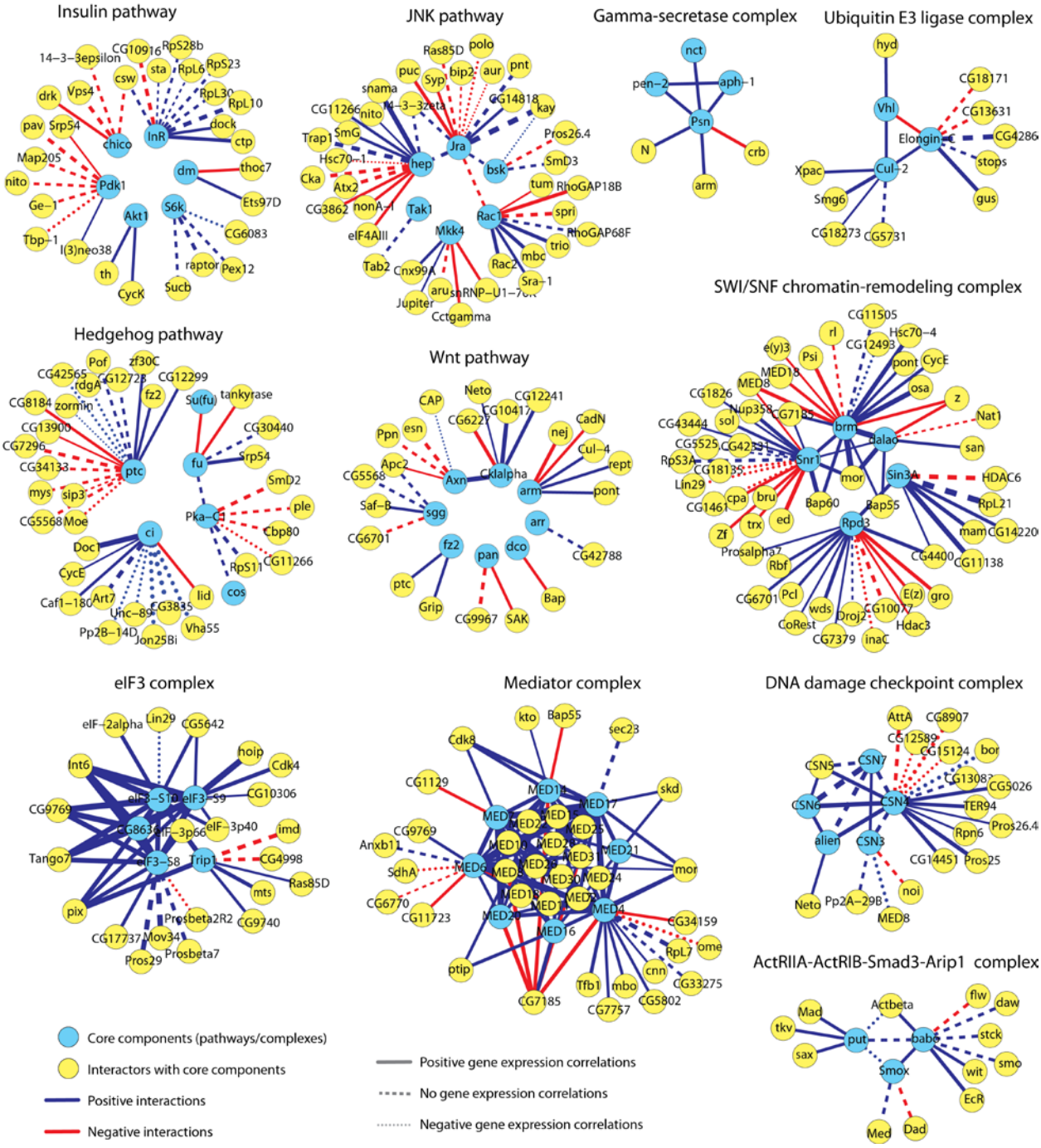

Supplementary Figure 8: Network representation of signed PPIs connecting known signaling pathways and protein complexes (Fig. 3 continued).

Nature Methods: doi:10.1038/nmeth.2733

Supplementary Figure 9

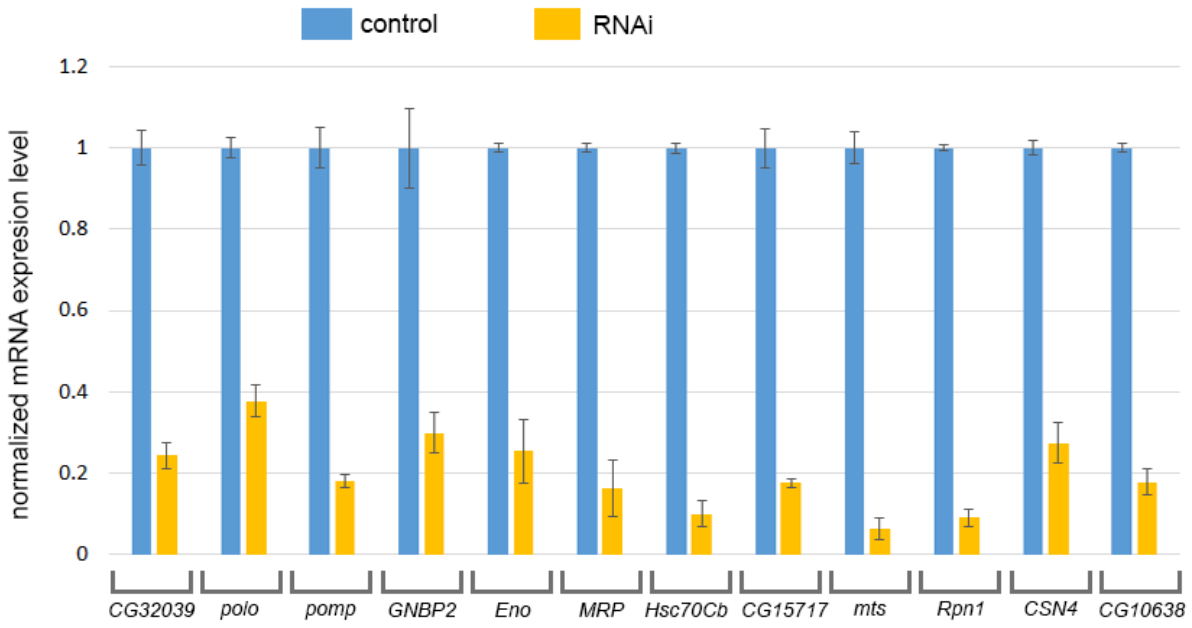

Supplementary Figure 9: Quantification of RNAi knockdown. mRNA expression levels following two days of knockdown in S2R+ cells were analyzed by quantitative RT-PCR (see experimental procedures). For each experiment, mRNA levels from knockdowns were normalized to lacZ RNAi controls. The following dsRNAs were used for knockdown: CG32039 (DRSC08982); polo (DRSC38944); Pomp (DRSC03201); GNBP2 (DRSC10404); Eno (DRSC00750); MRP (DRSC02942); Hsc70Cb (DRSC26538); CG15717 (DRSC34144); mts (DRSC03574); Rpn1 (DRSC32192); CSN4 (DRSC07350); CG10638 (DRSC42172). Error bars indicate the SEM.

Nature Methods: doi:10.1038/nmeth.2733

Supplementary Figure 10

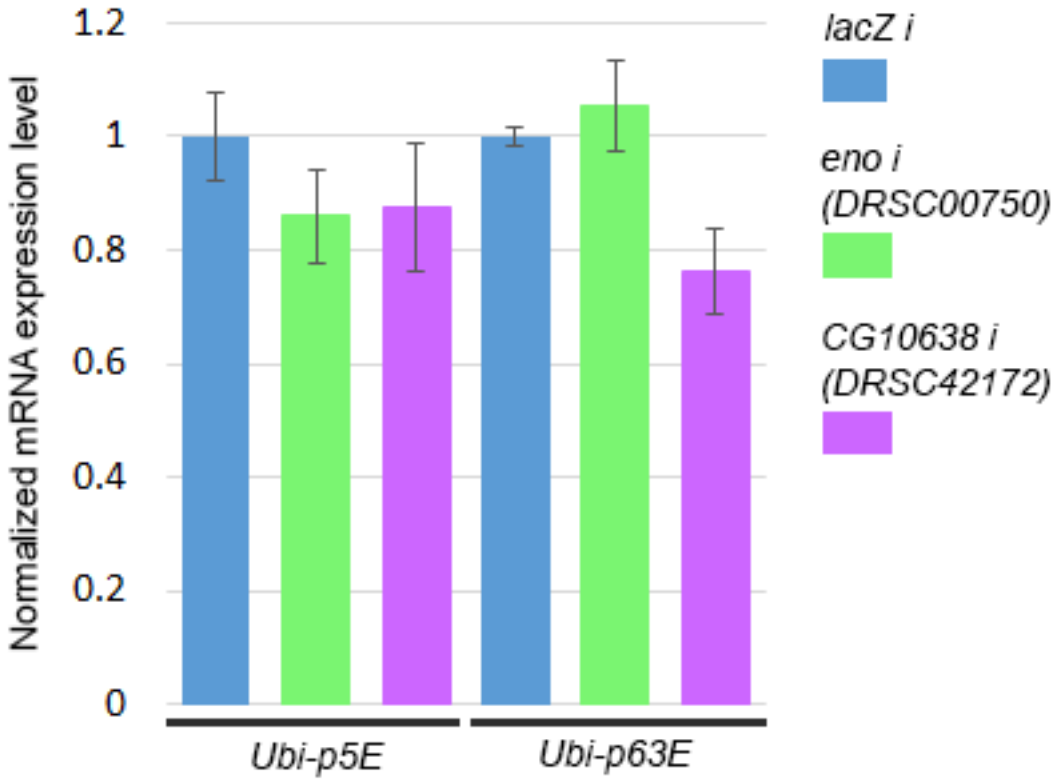

Supplementary Figure 10: Quantitation of ubiquitin expression. mRNA expression levels of two ubiquitin genes (Ubi-p5E and Ubi-p63E) following Eno (DRSC00750) or CG10638 (DRSC42172) knockdown. For each gene, mRNA levels after two days of knockdown in S2R+ cells were analyzed by quantitative RT-PCR, and normalized to lacZ RNAi controls. Knockdown of Eno or CG10638 had no significant effect on ubiquitin expression. Error bars indicate the SEM.

Nature Methods: doi:10.1038/nmeth.2733

Supplementary Figure 11

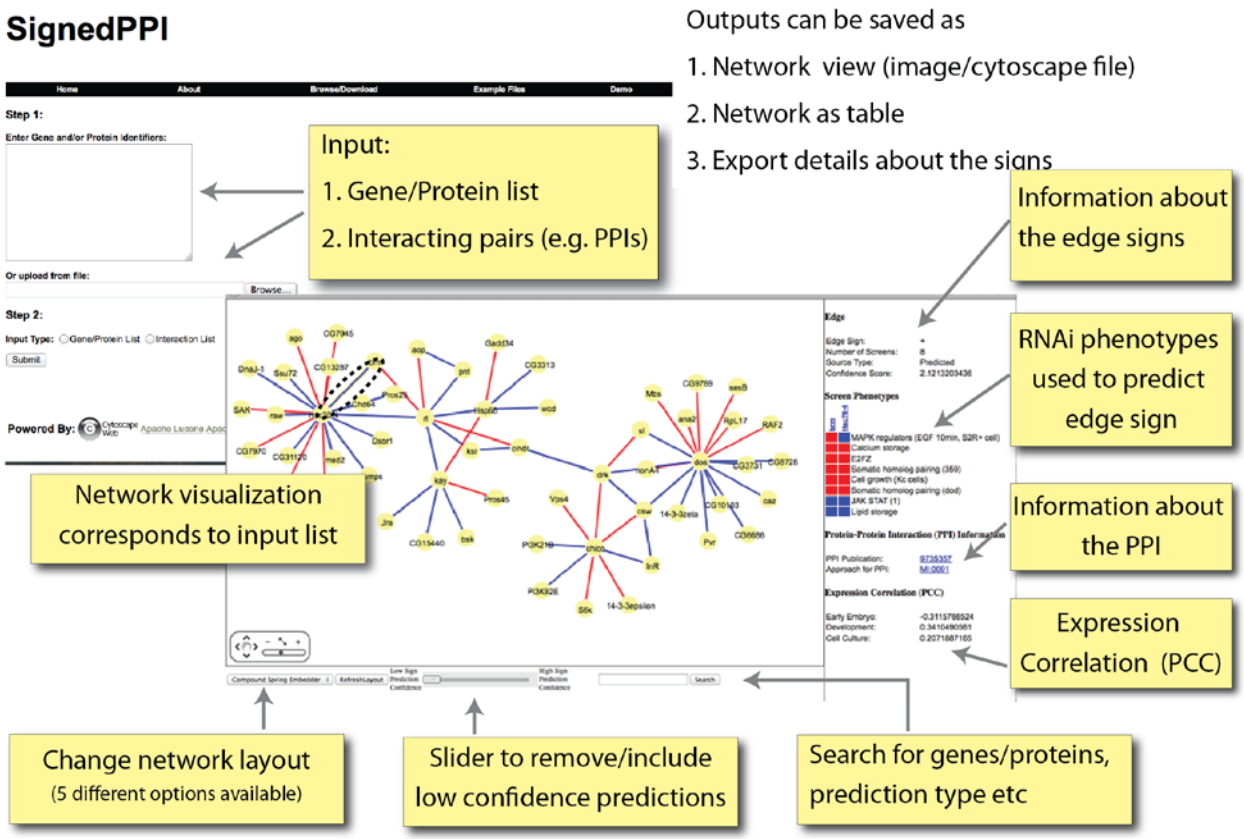

Supplementary Figure 11: Snapshot of the SignedPPI database. The features of input and output pages are highlighted. Users can query the database with a single gene, list of genes, proteins, a list of genes or proteins associated with experimental values (e.g. Z-score or fold-change values), or with a list of interacting pair of genes or proteins. Once the user uploads data, the tool generates a network with positive and negative interactions connecting the input list. To get more information about the edge signs, the user can click on the edges and the corresponding information including the phenotype vectors is displayed. To expand the network, the user can double click a node, which then adds direct neighbors to the selected node. The tool uses sign score as a function to zoom in or out of the network. For example, after zooming out, the tool displays only the core network with maximum sign score, whereas zooming in reveals more details on edges with moderate sign score. If the user uploads new *Drosophila* PPIs, the tool predicts signs based on the 49 RNAi screens stored in the server. In this case, instead of retrieving the stored signed PPI, signs are predicted for the user input data.

Nature Methods: doi:10.1038/nmeth.2733

Supplementary Table 1: List of RNAi screens used to construct the phenotypic matrix. The screens were collected from *Drosophila* RNAi Screening Center (DRSC)[1], GenomeRNAi[2], Neuroblasts Screen online database (IMBA – I)[3] and Bristle Screen online database (IMBA – II)[4].

#	Phenotypes	Number of genes with phenotype	References	Source databases
1	Wingless (1)	471	[5]	DRSC
2	Protein Secretion Gogi	660	[6]	DRSC
3	Cell Growth (S2R+ cells)	961	[7]	DRSC
4	Cell Growth (Kc cells)	1178	[7]	DRSC
5	MAPK regulators (EGF baseline, S2R+ cell)	2204	[8]	DRSC
6	MAPK regulators (EGF 10min, S2R+ cell)	1495	[8]	DRSC
7	MAPK regulators (EGF 10min, Kc167 cell)	2259	[8]	DRSC
8	MAPK regulators (EGF 30min, Kc167 cell)	2085	[8]	DRSC
9	MAPK regulators (Insulin baseline, S2R+ cell)	3140	[9]	DRSC
10	MAPK regulators (Insulin 10min, S2R+ cell)	2144	[9]	DRSC
11	Apoptotic regulators	1549	[10]	DRSC
12	CRYZ degradation	1557	[11]	DRSC
13	E2FZ	1604	[12]	DRSC
14	Hedgehog	1610	[13]	DRSC
15	JAK STAT (1)	1760	[14]	DRSC
16	Calcium storage	2100	[15]	DRSC
17	Calcium entry	3012	[16]	DRSC
18	Somatic homolog pairing (dod)	274	[10]	DRSC
19	Somatic homolog pairing (359)	234	[10]	DRSC
20	Wnt proteins secretion	17	[17]	GenomeRNAi
21	Hedgehog signaling (2)	19	[18]	GenomeRNAi
22	Toll dependent immune response	28	[19]	GenomeRNAi
23	Innate immunity (1)	29	[20]	GenomeRNAi
24	*B. melitensis* infection	61	[21]	GenomeRNAi
25	Wg pathway regulation (3)	63	[22]	GenomeRNAi

Nature Methods: doi:10.1038/nmeth.2733

26	JAK STAT pathway (2)	67	[23]	GenomeRNAi
27	Innate immunity (2)	115	[24]	GenomeRNAi
28	Akt TOR regulation	134	[25]	GenomeRNAi
29	Notch induced transcription	149	[26]	GenomeRNAi
30	*C. trachomatis* infection	219	[27]	GenomeRNAi
31	Methyl methanesulphonate	391	[28]	GenomeRNAi
32	Adiposity regulation	512	[29]	GenomeRNAi
33	Huntingtin aggregation	514	[30]	GenomeRNAi
34	Heat Nociception	720	[31]	GenomeRNAi
35	Notch pathway regulation	899	[32]	GenomeRNAi
36	PGN induced dJNK	993	[33]	GenomeRNAi
37	Serratia marcescens infection	1176	[34]	GenomeRNAi
38	Lipid Storage	5071	[35]	GenomeRNAi
39	Cell Size	272	[3]	IMBA – I
40	Cell Death	556	[3]	IMBA – I
41	Bristles loss/gain	667	[4]	IMBA – II
42	Bristles proliferation	1499	[4]	IMBA – II
43	Unpublished phenotype 1	837	[36], Neumuller et al., unpublished	Unpublished
44	Unpublished phenotype 2	1201	[36], Neumuller et al., unpublished	Unpublished
45	Unpublished phenotype 3	1236	[36], Neumuller et al., unpublished	Unpublished
46	Unpublished phenotype 4	1344	[36], Neumuller et al., unpublished	Unpublished
47	Unpublished phenotype 5	1392	[36], Neumuller et al., unpublished	Unpublished
48	Unpublished phenotype 6	1752	[36], Neumuller et al., unpublished	Unpublished
49	Unpublished phenotype 7	2014	[36], Neumuller et al., unpublished	Unpublished

Nature Methods: doi:10.1038/nmeth.2733

Supplementary Table 2: Signaling PPIs with known signs collected from three major signaling pathway databases. The pairs with two or more matching phenotypes in the phenotypic matrix were selected for validation. Each signaling PPI dataset was downloaded from the corresponding website and the database version corresponds to the March 2012 release.

Pathway databases	**Number of interactions with signs**	
	Total interactions	**Interactions with ≥ 2 matching phenotypes**
SignaLink[37] http://signalink.org/	220	85
KEGG[38] http://www.genome.jp/kegg/pathway.html	194	46
STKE http://stke.sciencemag.org/cm/	94	16

Nature Methods: doi:10.1038/nmeth.2733

Supplementary Table 3: List of 106 signaling PPIs used as reference interactions in PRS and NRS. Signaling PPIs with known signs are collected from three major signaling pathway databases. After compiling the reference PPIs, the signs are manually curated by checking with appropriate literature. The sign from source database, sign in PRS and NRS are shown.

Gene A	Gene B	Source Sign	Sign in PRS	Sign in NRS	Source
gish	Ci	-	-	+	KEGG
bib	Dl	+	+	-	SignaLink
Sara	Flw	+	+	-	SignaLink
dome	Hop	+	+	-	SignaLink
Atg12	Atg7	+	+	-	KEGG
Pten	Pdk1	-	-	+	SignaLink
Cas	C3G	+	+	-	STKE
slpr	Hep	+	+	-	SignaLink
PEK	eIF-2alpha	+	+	-	KEGG
Myt1	cdc2	-	-	+	KEGG
Mkk4	Bsk	+	+	-	SignaLink
sgg	Jra	-	-	+	SignaLink
sgg	Tim	+	+	-	STKE
Egfr	Shc	+	+	-	SignaLink
Egfr	Drk	+	+	-	KEGG;SignaLink
pnt	Br	-	-	+	KEGG
gig	Rheb	-	-	+	KEGG
phl	Hpo	-	-	+	SignaLink
phl	Dsor1	+	+	-	SignaLink
ksr	Phl	+	+	-	SignaLink
ci	Nej	+	+	-	SignaLink
ird5	Tsc1	-	-	+	KEGG
Akt1	S6k	+	+	-	SignaLink
Akt1	Gig	-	-	+	KEGG
Tab2	Tak1	+	+	-	SignaLink
Axn	Arm	-	-	+	STKE;SignaLink
tws	Akt1	-	-	+	SignaLink *
Su(var)2-10	Stat92E	-	-	+	KEGG;SignaLink
cno	Ras85D	-	-	+	SignaLink
Dl	N	+	+	-	KEGG;SignaLink
smo	Pka-C1	+	+	-	SignaLink
smo	Cos	-	-	+	STKE;SignaLink
Rheb	Tor	+	+	-	KEGG
H	N	-	-	+	SignaLink
rdgC	ninaE	+	+	-	KEGG
drk	Sos	+	+	-	KEGG;SignaLink
Gcn2	eIF-2alpha	+	+	-	KEGG
hh	Ptc	-	-	+	KEGG;STKE;SignaLink

Nature Methods: doi:10.1038/nmeth.2733

slmb	Arm	-	-	+	STKE;SignaLink
slmb	Ci	-	-	+	KEGG;STKE;SignaLink
Wnt10	fz2	+	+	-	KEGG
Pka-C1	CkIalpha	+	+	-	SignaLink
Pka-C1	Smo	+	+	-	SignaLink
mad2	fzr2	-	-	+	KEGG
csw	Phl	+	+	-	KEGG
scw	Sax	+	+	-	SignaLink
Ilp5	InR	+	+	-	STKE;SignaLink
Gap1	Ras85D	-	-	+	KEGG
fu	Ci	+	+	-	SignaLink
fu	Su(fu)	-	-	+	SignaLink
CkIalpha	Arm	-	-	+	STKE;SignaLink
CkIalpha	Slmb	+	+	-	SignaLink
aux	Dl	+	+	-	SignaLink
gbb	Sax	+	+	-	SignaLink
ttv	Hh	+	+	-	SignaLink
Sos	Ras85D	+	+	-	KEGG;SignaLink
Roc1a	Ci	-	-	+	SignaLink
Roc1a	Slmb	+	+	-	SignaLink
Pdk1	S6k	+	+	-	STKE
Pdk1	Akt1	+	+	-	STKE;SignaLink
bsk	Jra	+	+	-	SignaLink
Pk92B	Hep	+	+	-	KEGG
Shc	Drk	+	+	-	KEGG;SignaLink
sec15	Rab11	+	+	-	SignaLink
cnk	Phl	+	+	-	SignaLink
neur	Dl	+	+	-	SignaLink
upd2	Dome	+	+	-	SignaLink
nmo	Pan	-	-	+	SignaLink
Tom	Neur	-	-	+	SignaLink
Cul-3	Ci	-	-	+	SignaLink
hop	Stat92E	+	+	-	SignaLink
Rho1	Rok	+	+	-	KEGG
SNF1A	Tor	-	-	+	KEGG
CG9175	sar1	+	+	-	KEGG
lqf	Ser	+	+	-	SignaLink
sty	Gap1	+	+	-	SignaLink
Dsor1	Rl	+	+	-	KEGG;SignaLink
rl	Lk6	+	+	-	SignaLink
rl	Pnt	+	+	-	SignaLink
rl	Gig	-	-	+	KEGG
Su(H)	H	-	-	+	SignaLink *
star1	Spi	+	+	-	SignaLink
rasp	Spi	+	+	-	SignaLink
Psn	Arm	+	+	-	KEGG

Nature Methods: doi:10.1038/nmeth.2733

Psn	N	+	+	-	SignaLink
upd3	Dome	+	+	-	SignaLink
arm	Pan	+	+	-	STKE;SignaLink
pygo	Arm	+	+	-	STKE;SignaLink
wntD	fz2	+	+	-	KEGG
lin19	Slmb	+	+	-	SignaLink
Gprk1	ninaE	-	-	+	KEGG
Socs36E	Hop	-	-	+	KEGG;SignaLink
cos	Pka-C1	+	+	-	SignaLink
rl	Cic	-	-	+	SignaLink *
Atg8b	Atg7	+	+	-	KEGG
lin19	Ci	-	-	+	SignaLink
bib	N	+	+	-	SignaLink
S6k	Chico	-	-	+	KEGG
Cbl	Egfr	-	-	+	SignaLink
Akt1	Foxo	-	-	+	SignaLink
Stam	Hop	+	+	-	KEGG;SignaLink
Mkp3	Rl	-	-	+	SignaLink
nej	Pan	-	-	+	STKE;SignaLink
chico	Drk	+	+	-	SignaLink
H	CtBP	+	+	-	SignaLink
CkIIbeta	Per	-	-	+	STKE

* signs from original database is changed based on the literature curation.

Nature Methods: doi:10.1038/nmeth.2733

Supplementary Table 4: Validation of the performance using subsets of phenotype matrices. Number of PPIs in PRS and the performance (ROC area) are highlighted for each subset of RNAi screens.

Phenotype matrix	Number of interactions	ROC area under curve
Published	93	0.857
Unpublished	15	0.855
Combined	106	0.858

Supplementary Table 5: Performance of the classifiers trained to predict signs of interactions. Classifiers implemented in weka software[39] were used to train and test. All 49 RNAi screens were directly used as features. Note that poor performance of the classifiers could be due to sparseness of the phenotype matrix (missing values).

Classifiers	ROC area under curve from 10 fold cross validation	
	Positive interactions	Negative interactions
NaïveBayes	0.6	0.6
MultilayerPerceptron	0.657	0.67
RandomForest	0.65	0.695

Nature Methods: doi:10.1038/nmeth.2733

Supplementary Table 6: PPI datasets used to construct *Drosophila* integrated PPI network (MasterNet). Names of the datasets, publication references, URL, and number of PPIs and proteins in the dataset are listed. All the PPI datasets are downloaded from the corresponding website and the database version corresponds to the September 2012 release. In the integrated network the gene/protein identifiers from the corresponding databases are mapped to Flybase gene IDs.

PPI datasets	**Interactions**	**Proteins**
BioGrid[40] http://thebiogrid.org/	23916	7305
IntAct[41] http://www.ebi.ac.uk/intact/	25385	7530
DIP[42] http://dip.doe-mbi.ucla.edu/dip/Main.cgi	19753	6584
MINT[43] http://cbm.bio.uniroma2.it/mint/	17336	5917
DroID[44] http://www.droidb.org/	87070	9068
Drosophila AP-MS dataset (DPiM)[45] https://interfly.med.harvard.edu/	10964	2296
MasterNet (integrated network)	98500	9373
Network with potential direct interactions	47293	9107

Nature Methods: doi:10.1038/nmeth.2733

Supplementary Table 8: Functional enrichment analysis of hub proteins. Proteins with 5 or more interactions were considered hubs. Hubs were classified as: 1) hubs with primarily positive interactions (≥ 75% of interactions are positive interactions); 2) hubs with primarily negative interactions (≥ 75% of interactions are negative interactions); or 3) hubs with both positive and negative interactions. Gene Ontology functional enrichment analysis was performed with GO::TermFinder[46] and GO annotation was downloaded from GO database (excluding IEA annotations).

Hub type	GO ID	P-value	Number of genes	GO term
Hubs with primarily positive interactions	GO:0003712	5.76E-19	29	transcription cofactor activity
	GO:0016462	3.24E-16	57	pyrophosphatase activity
	GO:0004175	1.49E-08	35	endopeptidase activity
	GO:0008553	6.70E-08	14	hydrogen-exporting ATPase activity, phosphorylative mechanism
	GO:0042625	1.51E-06	15	ATPase activity, coupled to transmembrane movement of ions
	GO:0001104	1.86E-19	21	RNA polymerase II transcription cofactor activity
	GO:0008135	0.0003	12	translation factor activity, nucleic acid binding
	GO:0003682	0.0014	12	chromatin binding
	GO:0004672	0.0004	24	protein kinase activity
	GO:0019199	0.0014	7	transmembrane receptor protein kinase activity
	GO:0003678	0.0025	8	DNA helicase activity
	GO:0004579	0.0064	3	dolichyl-diphosphooligosaccharide-protein glycotransferase activity
	GO:0000983	0.0060	6	RNA polymerase II core promoter sequence-specific DNA binding transcription factor activity
	GO:0022890	0.0275	18	inorganic cation transmembrane transporter activity
	GO:0015405	0.0070	15	P-P-bond-hydrolysis-driven transmembrane transporter activity
	GO:0008233	7.72E-05	35	peptidase activity
	GO:0004386	0.0172	12	helicase activity
	GO:0070011	4.55E-05	35	peptidase activity, acting on L-amino acid peptides
	GO:0042813	5.55E-06	5	Wnt-activated receptor activity
	GO:0005024	0.0009	4	transforming growth factor beta-activated receptor activity
	GO:0003743	0.0214	8	translation initiation factor activity
Hubs with primarily negative interactions	GO:0003714	0.0025	3	transcription corepressor activity
	GO:0003735	0.0050	6	structural constituent of ribosome

Nature Methods: doi:10.1038/nmeth.2733

Hubs with both positive and negative interactions	GO:0003735	4.53E-09	24	structural constituent of ribosome
	GO:0003729	2.90E-08	20	mRNA binding
	GO:0004672	4.42E-08	23	protein kinase activity
	GO:0004674	1.00E-07	19	protein serine/threonine kinase activity
	GO:0016773	1.79E-06	23	phosphotransferase activity, alcohol group as acceptor
	GO:0008092	1.95E-05	17	cytoskeletal protein binding
	GO:0019787	0.0323	7	small conjugating protein ligase activity
	GO:0005523	0.0008	3	tropomyosin binding
	GO:0004712	0.0009	4	protein serine/threonine/tyrosine kinase activity
	GO:0016772	2.77E-05	25	transferase activity, transferring phosphorus-containing groups
	GO:0003724	0.0341	6	RNA helicase activity
	GO:0016538	0.0013	5	cyclin-dependent protein kinase regulator activity
	GO:0008026	0.0047	8	ATP-dependent helicase activity
	GO:0070035	0.0047	8	purine NTP-dependent helicase activity
	GO:0003779	0.0206	9	actin binding
	GO:0019887	0.0381	6	protein kinase regulator activity
	GO:0019207	0.0472	6	kinase regulator activity

Nature Methods: doi:10.1038/nmeth.2733

Supplementary Table 9: Enrichment analysis of triad motifs using FANMOD tool[47]. FANMOD was downloaded from http://theinf1.informatik.uni-jena.de/~wernicke/motifs/ and locally installed. The signed PPI is used as input and network treated as colored edges. Enrichment analysis for sub graph size 3 against 1000 random network (default values are used for other parameters).

Motif	Frequency (Real network)	Mean Frequency (Random network)	Standard Deviation (Random network)	Z-Score	p-value
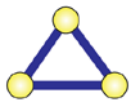	7.1746%	0.0023557%	3.5649e-005	2011.9	0
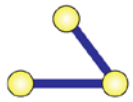	43.715%	56.427%	6.6871e-005	-1901	1
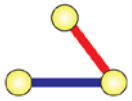	36.951%	33.212%	6.516e-005	573.82	0
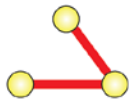	11.359%	10.346%	2.2643e-005	447.41	0
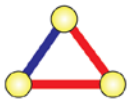	0.60048%	0.0035386%	2.4485e-005	243.8	0
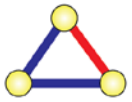	0.187%	0.0085829%	4.0937e-005	43.584	0
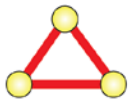	0.012467%	6.6335e-005%	3.6602e-006	33.879	0

Nature Methods: doi:10.1038/nmeth.2733

Supplementary Table 11: Conserved and disease-related signed PPIs

Interactions	Total PPIs	Conserved interactions		Potential interolog		Not conserved	
		PPIs	Percent	PPIs	Percent	PPIs	Percent
All PPIs	6125	1006	16.4%	4431	72.3%	688	11.2%
Disease PPIs	2024	321	15.8%	1567	77.4%	136	6.7%

Supplementary Table 12: Results from RNAi screen in *Drosophila* primary embryonic muscle cells.

Gene Symbol	**Amplicon ID**	**Replicates**				**Median Value**	**Comments**
		1	**2**	**3**	**4**		
Chc	DRSC34418	0.840	0.628	0.596	0.424	0.612	Positive regulator
	DRSC34419	0.599	0.777	0.409	0.603	0.601	
	DRSC20229	-0.263	-0.214	-0.379	-0.280	-0.271	
Spindly	DRSC31559	-0.087	0.154	-0.219	-0.269	-0.153	Not scored
	DRSC31558	0.053	0.220	0.058	-0.334	0.055	
	DRSC00430	0.131	-0.033	0.247	-0.354	0.049	
Tbp-1	DRSC33361	0.196	0.241	0.240	0.218	0.229	Core component
	DRSC26269	0.743	0.661	0.565	0.686	0.673	
	DRSC16842	0.774	0.906	0.833	0.494	0.803	
	DRSC33360	0.732	1.084	0.550	0.851	0.792	
Pros29	DRSC32170	0.884	1.094	0.675	0.783	0.833	Core component
	DRSC04644	0.786	0.571	0.549	0.289	0.560	
	DRSC32171	1.199	0.724	0.825	0.616	0.774	
CG32039	DRSC08982	-0.291	-0.319	-0.367	-0.622	-0.343	Negative regulator
	DRSC35191	-0.577	-0.636	-0.820	-0.965	-0.728	
	DRSC28597	-0.709	-0.700	-0.876	-0.670	-0.705	

Nature Methods: doi:10.1038/nmeth.2733

Prosalpha5	DRSC32184	0.138	0.328	0.045	-0.468	0.091	Core component
	DRSC32185	0.859	0.520	0.422	0.639	0.580	
	DRSC07514	0.670	0.686	0.417	0.455	0.563	
Rpn7	DRSC25951	0.610	0.813	1.070	0.965	0.889	Core component
	DRSC32204	0.723	1.010	0.572	0.342	0.647	
	DRSC32205	0.359	0.339	0.144	-0.543	0.241	
	DRSC16841	0.634	0.743	0.837	0.850	0.790	
CG17331	DRSC31563	0.655	0.524	0.365	0.522	0.523	Core component
	DRSC02603	0.578	0.617	0.337	0.430	0.504	
	DRSC31562	0.222	0.475	-0.320	0.196	0.209	
Cdk4	DRSC30791	-0.539	-0.509	-0.469	-0.532	-0.521	No clear phenotype
	DRSC07358	0.432	0.669	-0.137	0.208	0.320	
	DRSC30790	-0.137	-0.078	-0.343	-0.221	-0.179	
	DRSC27263	-0.558	-0.505	-0.488	-	-0.505	
polo	DRSC11384	-0.760	0.129	-0.175	0.082	-0.046	Positive regulator
	DRSC34464	0.037	0.070	0.151	-0.315	0.054	
	DRSC38944	0.436	0.577	0.539	0.424	0.487	
	DRSC37001	0.624	0.723	0.596	0.450	0.610	
	DRSC34463	0.581	0.960	0.418	0.642	0.611	
	DRSC22359	0.754	0.515	-0.098	0.540	0.527	
Prosbeta3	DRSC16801	0.515	0.769	0.466	0.601	0.558	Core component
	DRSC32181	0.661	0.769	0.754	0.660	0.707	
	DRSC32180	0.809	1.230	0.800	0.825	0.817	
	DRSC38439	0.875	0.858	0.785	0.395	0.822	
Rpn3	DRSC32101	0.048	0.102	0.266	-0.083	0.075	Core component
	DRSC32102	0.965	0.787	0.961	0.600	0.874	
	DRSC03318	0.671	0.806	0.662	0.435	0.667	
	DRSC29446	0.198	-0.016	0.226	-0.181	0.091	
Rpn2	DRSC32199	0.713	0.654	0.618	0.711	0.683	Core component
	DRSC16839	0.787	1.121	1.005	-0.814	0.896	
	DRSC38457	0.816	1.229	0.916	0.542	0.866	
	DRSC38456	1.069	0.829	0.702	0.749	0.789	
	DRSC32198	0.091	0.055	-0.033	0.135	0.073	
Prosalpha7	DRSC29365	0.760	0.412	0.595	0.640	0.617	Core component
	DRSC32177	0.803	0.899	0.561	0.790	0.797	
	DRSC32176	0.270	0.201	-0.143	0.447	0.236	
	DRSC07516	0.085	0.381	-0.151	0.207	0.146	
Pomp	DRSC32165	0.544	0.525	0.337	0.532	0.529	Positive regulator
	DRSC27581	-0.145	0.276	-0.082	-0.045	-0.064	
	DRSC03201	0.797	0.561	0.436	0.606	0.584	
Pros54	DRSC32175	0.611	0.770	0.794	0.552	0.690	Core component
	DRSC32174	0.731	0.711	0.594	0.338	0.652	
	DRSC11876	1.144	0.893	0.649	0.654	0.774	
Pros35	DRSC32173	0.697	0.812	0.496	0.259	0.596	Core component
	DRSC32172	0.662	0.599	0.518	0.643	0.621	
	DRSC03401	0.845	0.910	0.665	0.758	0.802	

Nature Methods: doi:10.1038/nmeth.2733

Rpt3	DRSC23412	0.700	0.732	0.636	0.491	0.668	Core component
	DRSC32208	0.372	-0.097	-0.225	0.170	0.036	
	DRSC20283	0.317	0.270	0.008	0.304	0.287	
	DRSC32209	0.996	0.918	0.660	0.553	0.789	
RpL40	DRSC31664	-0.671	-0.655	-0.579	-0.738	-0.663	Negative regulator
	DRSC42173	-0.519	-0.418	-0.679	-0.643	-0.581	
	DRSC00782	0.285	0.203	0.210	0.481	0.248	
GNBP2	DRSC42164	-0.091	0.086	0.456	0.209	0.147	Not scored
	DRSC10404	0.072	0.489	-0.009	0.108	0.090	
	DRSC42165	0.469	0.204	-0.395	0.229	0.217	
Pros25	DRSC32166	0.507	0.840	0.453	0.689	0.598	Core component
	DRSC16798	0.147	-3.305	-0.417	-0.629	-0.523	
	DRSC28078	0.279	0.336	-0.429	0.205	0.242	
	DRSC32167	0.179	0.776	0.271	0.191	0.231	
Rpn6	DRSC32203	0.431	-0.225	-0.277	0.082	-0.071	Core component
	DRSC07541	0.563	0.621	0.444	0.309	0.503	
	DRSC32202	0.799	0.885	0.888	0.834	0.860	
Pros26.4	DRSC16799	0.753	0.842	0.425	0.647	0.700	Core component
	DRSC25012	0.355	0.706	0.304	0.359	0.357	
	DRSC32051	1.053	1.033	0.543	0.639	0.836	
	DRSC32052	0.848	0.915	0.740	0.676	0.794	
Eno	DRSC00750	0.257	0.013	0.325	-0.461	0.135	Positive regulator
	DRSC42167	0.573	0.510	0.114	-0.226	0.312	
	DRSC42166	0.535	0.602	0.419	0.364	0.477	
Prosbeta5	DRSC28939	0.099	0.235	0.202	0.110	0.156	Core component
	DRSC07517	0.905	0.990	0.962	0.682	0.934	
	DRSC32182	0.461	0.403	0.335	0.263	0.369	
	DRSC32183	0.599	1.135	0.808	0.561	0.704	
MRP	DRSC39503	-0.946	-1.101	-0.946	-0.925	-0.946	Negative regulator
	DRSC39210	-0.310	-0.350	-0.519	-0.420	-0.385	
	DRSC02942	-0.528	-0.660	-0.575	-0.464	-0.552	
	DRSC40861	-0.211	-0.474	-0.445	-0.413	-0.429	
ATPsyn-beta	DRSC40683	0.022	0.073	-0.211	-0.304	-0.095	Not scored
	DRSC34212	0.281	0.355	-0.228	0.155	0.218	
	DRSC40016	0.072	0.278	-0.170	0.315	0.175	
	DRSC17194	-0.541	-0.249	-0.352	-0.280	-0.316	
Hsc70Cb	DRSC11186	0.391	0.565	0.110	0.388	0.389	Positive regulator
	DRSC26538	0.433	0.312	0.481	0.263	0.373	
	DRSC34558	0.711	0.652	0.337	0.109	0.495	
	DRSC34557	0.725	0.602	0.159	0.505	0.554	
Rpn12	DRSC32197	0.602	0.724	0.465	0.509	0.556	Core component
	DRSC32196	0.642	0.593	0.433	0.458	0.525	
	DRSC28589	0.559	1.041	0.976	0.472	0.768	
	DRSC11275	0.226	0.248	0.300	-0.130	0.237	
Rpt4	DRSC32210	-0.012	0.260	-0.173	-0.188	-0.093	Core component
	DRSC32211	-0.080	-0.067	-0.084	-0.154	-0.082	

Nature Methods: doi:10.1038/nmeth.2733

	DRSC18713	0.813	0.536	0.436	0.582	0.559	
Prosbeta7	DRSC32030	0.335	0.607	0.135	0.115	0.235	Core component
	DRSC32029	0.790	0.676	0.637	0.584	0.657	
	DRSC12186	0.240	0.568	-0.029	0.456	0.348	
Mov34	DRSC29897	1.190	1.415	0.750	0.642	0.970	Core component
	DRSC04624	0.577	0.789	0.486	0.835	0.683	
	DRSC32154	0.764	0.600	0.671	0.761	0.716	
	DRSC32153	0.909	0.969	0.596	0.531	0.753	
Pros26	DRSC32169	0.249	0.136	0.345	0.286	0.267	Core component
	DRSC32168	1.030	1.000	0.590	0.757	0.878	
	DRSC11256	0.327	0.413	0.231	0.081	0.279	
Rpn5	DRSC12367	0.833	0.905	0.610	0.627	0.730	Core component
	DRSC32201	0.805	1.256	0.831	0.994	0.912	
	DRSC32200	0.675	0.792	0.486	0.554	0.614	
	DRSC28279	0.595	0.701	0.958	0.338	0.648	
Drep-4	DRSC03408	0.172	0.161	0.163	-0.337	0.162	Not scored
	DRSC42168	0.252	0.216	-0.450	0.448	0.234	
	DRSC42169	0.196	0.326	-0.399	0.214	0.205	
CG15717	DRSC34144	-0.450	-0.161	-0.599	-0.465	-0.457	Negative regulator
	DRSC19684	-0.513	-0.497	-0.530	-0.570	-0.522	
	DRSC34145	-0.254	0.487	0.028	0.275	0.152	
Rpn9	DRSC32207	0.894	0.712	0.964	0.747	0.820	Core component
	DRSC27177	1.085	1.330	1.131	0.689	1.108	
	DRSC32206	0.327	0.250	0.311	-0.349	0.280	
	DRSC16840	0.329	0.188	-0.009	-0.232	0.090	
Rpt1	DRSC30799	0.384	0.614	0.077	-0.109	0.231	Core component
	DRSC07542	1.093	1.291	0.782	0.436	0.937	
	DRSC30800	0.210	0.473	-0.029	-0.053	0.090	
Prosbeta2	DRSC32179	0.772	0.725	0.865	0.427	0.749	Core component
	DRSC32178	1.626	1.211	0.818	0.951	1.081	
	DRSC11257	0.636	0.607	0.743	0.755	0.690	
mts	DRSC36626	-0.147	0.100	-0.151	-0.304	-0.149	Not scored
	DRSC03574	0.314	0.417	-0.614	0.093	0.203	
	DRSC30715	0.199	0.245	0.282	0.036	0.222	
	DRSC30716	0.027	-0.154	-0.707	0.190	-0.064	
Rpn1	DRSC32193	0.565	0.696	1.033	0.562	0.630	Core component
	DRSC32192	0.543	0.483	0.340	0.362	0.422	
	DRSC11274	0.676	1.031	0.695	0.332	0.685	
	DRSC38454	0.978	0.993	0.880	0.577	0.929	
Cpr11A	DRSC19861	-0.055	-0.279	-0.660	-0.121	-0.200	Not scored
	DRSC26786	-0.007	0.022	-0.045	0.187	0.007	
	DRSC42174	0.152	-0.126	-0.285	0.258	0.013	
CG17829	DRSC24069	0.459	0.546	0.379	0.395	0.427	Not scored
	DRSC18484	0.259	0.265	-0.511	0.042	0.151	
	DRSC42177	-0.168	0.361	0.023	0.189	0.106	
Prosbeta1	DRSC32139	0.713	0.758	0.612	0.681	0.697	Core

Nature Methods: doi:10.1038/nmeth.2733

	DRSC07159	0.773	0.974	0.794	0.442	0.783	component
	DRSC32140	0.371	0.311	-0.443	0.672	0.341	
CG5792	DRSC28212	0.007	-0.147	-0.486	-0.743	-0.317	Not scored
	DRSC42176	-0.120	-0.408	-0.581	0.313	-0.264	
	DRSC41068	0.101	0.494	0.016	0.339	0.220	
	DRSC02897	0.051	-0.109	0.047	-0.322	-0.031	
TER94	DRSC41049	0.219	0.413	0.247	-0.298	0.233	Core component
	DRSC07560	0.689	0.591	0.834	0.235	0.640	
	DRSC32221	0.443	0.219	0.346	0.297	0.322	
	DRSC32220	0.805	0.716	0.572	0.508	0.644	
	DRSC27600	0.435	0.416	0.310	0.437	0.425	
CSN4	DRSC33300	0.498	-0.030	-0.460	0.224	0.097	Not scored
	DRSC07350	0.133	0.073	-0.471	-0.366	-0.147	
	DRSC33301	-0.324	-0.156	-0.132	-0.033	-0.144	
CG10638	DRSC42172	-0.245	-0.469	-0.305	-0.596	-0.387	Negative regulator
	DRSC09762	-0.732	-0.673	-0.616	-0.873	-0.703	
	DRSC29762	-0.379	-0.143	-0.687	-0.440	-0.409	
CG6415	DRSC02954	-0.031	0.308	-0.154	-0.148	-0.090	Not scored
	DRSC29833	0.140	0.055	-0.002	0.010	0.033	
	DRSC42175	0.378	0.246	0.286	0.264	0.275	
CG13349	DRSC42170	0.277	-0.387	-0.220	0.113	-0.054	Not scored
	DRSC06379	0.111	0.476	0.171	0.084	0.141	
	DRSC42171	0.068	0.351	0.414	-0.277	0.210	
Rpn11	DRSC32194	0.977	1.203	0.817	0.536	0.897	Core component
	DRSC32195	1.531	1.012	0.743	0.519	0.878	
	DRSC03422	1.000	0.734	0.545	0.664	0.699	
	DRSC38455	0.853	1.430	0.767	1.068	0.960	

Nature Methods: doi:10.1038/nmeth.2733

Supplementary Table 13: Results from the proteasome activity assay. The values correspond to log2 fold change over lacZ control.

Gene Symbol	Amplicon ID	Replicates				Median Value	P value
		1	2	3	4		
CG10638	DRSC09762	0.2841	0.6287	0.6479	0.4436	0.5391	0.0022
	DRSC29762	0.2240	0.4098	0.5796	0.1973	0.3199	0.0126
	DRSC42172	0.0144	0.1618	0.4204	0.3062	0.2358	0.0484
CG15717	DRSC19684	0.1212	0.2495	0.3108	0.1088	0.1868	0.0093
	DRSC34144	0.0255	0.0325	0.3722	-0.2302	0.0290	0.6267
	DRSC34145	0.1570	-0.2003	0.0457	-0.1568	-0.0520	0.7235
CG32039	DRSC08982	0.0326	0.1731	0.1051	0.2093	0.1395	0.0175
	DRSC28597	-0.0162	-0.4545	-0.2218	-0.4007	-0.3085	0.0295
	DRSC35191	0.2927	0.4758	0.2706	0.2704	0.2817	0.0012
MRP	DRSC02942	0.0973	0.5699	0.3237	0.3835	0.3539	0.0174
	DRSC40861	0.0707	-0.0893	0.2595	0.0122	0.0417	0.4026
	DRSC39503	0.2887	0.3296	0.3379	0.2126	0.3093	0.0001
	DRSC39210	0.5033	0.4273	0.3471	0.4398	0.4336	0.0000
Eno	DRSC00750	-0.6287	-0.8382	-0.5079	-0.7479	-0.6871	2.09E-05
	DRSC42167	-0.3286	-0.4528	-0.3435	-0.5163	-0.3971	4.18E-05
	DRSC42166	-0.6188	-0.6185	-0.1299	-0.2303	-0.4114	0.0142
Hsc70Cb	DRSC11186	-0.2537	-0.1110	-0.3177	-0.4216	-0.2854	0.0039
	DRSC26538	0.2459	-0.0593	0.0231	-0.0957	-0.0176	0.6808
	DRSC34558	-0.4697	0.2308	0.0414	0.1012	0.0716	0.9947
	DRSC34557	-0.0293	0.1499	0.0116	-0.1318	-0.0087	0.0335
polo	DRSC37001	-0.0710	-0.2135	-0.3155	-0.1625	-0.1878	0.0076
	DRSC38944	0.0350	-0.1888	0.2970	-0.0532	-0.0084	0.7629
	DRSC34464	-0.3006	-0.1035	0.0466	-0.3147	-0.1986	0.1013
	DRSC34463	-0.4443	-0.4985	-0.3641	-0.4038	-0.4239	2.35E-06
Pomp	DRSC03201	-0.8766	-0.5310	-0.9858	-1.0496	-0.9302	8.07E-05
	DRSC27581	-0.5231	-0.2902	-0.5531	-0.6327	-0.5380	0.0002
	DRSC32165	-0.7480	-0.2135	-0.4519	-0.6385	-0.5422	0.0025
Rpn1	DRSC11274	-1.1671	-1.2649	-0.6244	-0.9095	-1.0325	8.38E-05
	DRSC38454	-0.6819	-0.4693	-0.5310	-0.5294	-0.5302	5.26E-06
	DRSC32193	-0.7534	-1.1123	-0.6438	-0.4913	-0.6976	0.0003
	DRSC32192	-0.3215	-0.4077	-0.0463	-0.3154	-0.3184	0.0116
CSN4	DRSC07350	-0.2470	-0.1476	-0.0677	-0.4086	-0.1964	0.0193
	DRSC33300	0.0224	0.1258	-0.0556	0.1304	0.0750	0.2477
	DRSC33301	0.1085	0.0781	0.3506	0.0482	0.0934	0.0932
GNBP2	DRSC10404	-0.5036	-0.2032	-0.1837	-0.0098	-0.1935	0.0586
	DRSC42164	0.0279	-0.0482	0.4554	-0.0852	-0.0096	0.4809
	DRSC42165	0.1628	0.1881	-0.0335	0.0181	0.0922	0.1689
mts	DRSC03574	0.0653	0.1820	0.5003	0.2541	0.2185	0.0459
	DRSC36626	-0.1323	0.0485	-0.4629	-0.2925	-0.2102	0.1013
	DRSC30715	-0.1026	-0.2135	-0.1919	-0.4807	-0.2026	0.0154
	DRSC30716	-0.3644	-0.0495	-0.9699	0.1579	-0.1984	0.2724

Nature Methods: doi:10.1038/nmeth.2733

Supplementary Table 14: Details of PPIs connecting proteasome complex and novel proteasome regulators identified. ID1 and ID2 correspond to proteasome regulators and proteasome components, respectively. TAP: tandem affinity purification, Y2H: yeast two-hybrid

ID1	ID2	Sign	Score	Screens	Coexpress	PPI Assay	PPI PubMed	Human ortholog
Eno	Prosbeta5	+	1.73	3	-0.06	TAP	22036573	ENO1
polo	Pros25	+	2.23	5	0.26	Y2H	14605208	PLK1
Hsc70Cb	Pros54	+	2.20	5	0.19	TAP	15946124	HSPA4
Hsc70Cb	TER94	+	1.73	3	0.33	TAP	22036573	HSPA4
Pomp	Prosalpha7	+	3	9	0.97	TAP	22036573	POMP
Pomp	Prosbeta2R2	+	1	4	0.16	TAP	22036573	POMP
Pomp	Rpt3	+	3.46	12	0.79	TAP	22036573	POMP
Pomp	Pros35	+	2.33	9	0.92	TAP	22036573	POMP
Pomp	Pros29	+	1.63	6	0.94	TAP	22036573	POMP
Pomp	Pros25	+	2.11	11	0.96	TAP	22036573	POMP
Pomp	Prosbeta7	+	2.88	12	0.94	TAP	22036573	POMP
Pomp	Rpt1	+	2.33	9	0.87	TAP	22036573	POMP
Pomp	Pros26.4	+	3.31	11	0.90	TAP	22036573	POMP
Pomp	Rpn1	+	3.16	10	0.79	TAP	22036573	POMP
Pomp	Prosbeta3	+	3.16	10	0.98	TAP	22036573	POMP
Pomp	Rpt4	+	3.16	10	0.90	TAP	22036573	POMP
Pomp	Prosbeta1	+	2.30	12	0.96	TAP	22036573	POMP
Pomp	Prosbeta5	+	2.52	10	0.95	TAP	22036573	POMP
Pomp	Tbp-1	+	2.88	12	0.73	TAP	22036573	POMP
Pomp	Rpn2	+	2.30	12	0.82	TAP	22036573	POMP
Pomp	Pros26	+	3.31	11	0.95	TAP	22036573	POMP
Pomp	Prosbeta2	+	3.31	11	0.91	TAP	22036573	POMP
Pomp	CG17331	+	2.52	10	0.95	TAP	22036573	POMP
Pomp	Prosalpha5	+	3.16	10	0.98	TAP	22036573	POMP
CG10638	TER94	-	-1.73	3	0.57	TAP	22036573	AKR1D1
CG10638	Pros35	-	-1.73	3	0.483	TAP	22036573	AKR1D1
CG15717	Prosalpha7	-	-2	4	-0.17	TAP	22036573	ALDH16A1
CG15717	Prosbeta3	-	-1.73	3	-0.21	TAP	22036573	ALDH16A1
CG15717	Prosbeta1	-	-1.73	3	-0.26	TAP	22036573	ALDH16A1
CG15717	Pros35	-	-1.73	3	-0.07	TAP	22036573	ALDH16A1
CG15717	Pros25	-	-1	4	-0.19	TAP	22036573	ALDH16A1
CG15717	Prosbeta7	-	-1.73	3	-0.18	TAP	22036573	ALDH16A1
CG15717	Prosbeta5	-	-2	4	-0.10	TAP	22036573	ALDH16A1
CG15717	Pros26	-	-1.73	3	-0.24	TAP	22036573	ALDH16A1
CG15717	Prosbeta2	-	-1.73	3	-0.12	TAP	22036573	ALDH16A1
CG32039	TER94	-	-1.5	1	0.62	-	-	SVIP
MRP	Rpt1	-	-2	4	-0.46	TAP	22036573	ABCC3
MRP	Rpn1	-	-1.73	3	-0.42	TAP	22036573	ABCC3
MRP	TER94	-	-1.73	3	-0.52	TAP	22036573	ABCC3

Nature Methods: doi:10.1038/nmeth.2733

References

1. Flockhart, I.T. et al. FlyRNAi.org--the database of the Drosophila RNAi screening center: 2012 update. *Nucleic Acids Res* **40**, D715-719 (2012).
2. Gilsdorf, M. et al. GenomeRNAi: a database for cell-based RNAi phenotypes. 2009 update. *Nucleic Acids Res* **38**, D448-452 (2010).
3. Neumuller, R.A. et al. Genome-wide analysis of self-renewal in Drosophila neural stem cells by transgenic RNAi. *Cell Stem Cell* **8**, 580-593 (2011).
4. Mummery-Widmer, J.L. et al. Genome-wide analysis of Notch signalling in Drosophila by transgenic RNAi. *Nature* **458**, 987-992 (2009).
5. DasGupta, R., Kaykas, A., Moon, R.T. & Perrimon, N. Functional genomic analysis of the Wnt-wingless signaling pathway. *Science* **308**, 826-833 (2005).
6. Bard, F. et al. Functional genomics reveals genes involved in protein secretion and Golgi organization. *Nature* **439**, 604-607 (2006).
7. Boutros, M. et al. Genome-wide RNAi analysis of growth and viability in Drosophila cells. *Science* **303**, 832-835 (2004).
8. Friedman, A.A. et al. Proteomic and functional genomic landscape of receptor tyrosine kinase and ras to extracellular signal-regulated kinase signaling. *Science signaling* **4**, rs10 (2011).
9. Friedman, A. & Perrimon, N. A functional RNAi screen for regulators of receptor tyrosine kinase and ERK signalling. *Nature* **444**, 230-234 (2006).
10. Yi, C.H. et al. A genome-wide RNAi screen reveals multiple regulators of caspase activation. *J Cell Biol* **179**, 619-626 (2007).
11. Sathyanarayanan, S. et al. Identification of novel genes involved in light-dependent CRY degradation through a genome-wide RNAi screen. *Genes Dev* **22**, 1522-1533 (2008).
12. Lu, J., Ruhf, M.L., Perrimon, N. & Leder, P. A genome-wide RNA interference screen identifies putative chromatin regulators essential for E2F repression. *Proc Natl Acad Sci U S A* **104**, 9381-9386 (2007).
13. Nybakken, K., Vokes, S.A., Lin, T.Y., McMahon, A.P. & Perrimon, N. A genome-wide RNA interference screen in Drosophila melanogaster cells for new components of the Hh signaling pathway. *Nat Genet* **37**, 1323-1332 (2005).
14. Baeg, G.H., Zhou, R. & Perrimon, N. Genome-wide RNAi analysis of JAK/STAT signaling components in Drosophila. *Genes Dev* **19**, 1861-1870 (2005).
15. Zhang, S.L. et al. Genome-wide RNAi screen of Ca(2+) influx identifies genes that regulate Ca(2+) release-activated Ca(2+) channel activity. *Proc Natl Acad Sci U S A* **103**, 9357-9362 (2006).
16. Vig, M. et al. CRACM1 is a plasma membrane protein essential for store-operated Ca2+ entry. *Science* **312**, 1220-1223 (2006).
17. Buechling, T., Chaudhary, V., Spirohn, K., Weiss, M. & Boutros, M. p24 proteins are required for secretion of Wnt ligands. *EMBO Rep* **12**, 1265-1272 (2011).
18. Lum, L. et al. Identification of Hedgehog pathway components by RNAi in Drosophila cultured cells. *Science* **299**, 2039-2045 (2003).
19. Kuttenkeuler, D. et al. A large-scale RNAi screen identifies Deaf1 as a regulator of innate immune responses in Drosophila. *J Innate Immun* **2**, 181-194 (2010).
20. Kleino, A. et al. Inhibitor of apoptosis 2 and TAK1-binding protein are components of the Drosophila Imd pathway. *EMBO J* **24**, 3423-3434 (2005).
21. Qin, Q.M. et al. RNAi screen of endoplasmic reticulum-associated host factors reveals a role for IRE1alpha in supporting Brucella replication. *PLoS Pathog* **4**, e1000110 (2008).
22. Port, F., Hausmann, G. & Basler, K. A genome-wide RNA interference screen uncovers two p24 proteins as regulators of Wingless secretion. *EMBO Rep* **12**, 1144-1152 (2011).

Nature Methods: doi:10.1038/nmeth.2733

23. Muller, P., Kuttenkeuler, D., Gesellchen, V., Zeidler, M.P. & Boutros, M. Identification of JAK/STAT signalling components by genome-wide RNA interference. *Nature* **436**, 871-875 (2005).
24. Foley, E. & O'Farrell, P.H. Functional dissection of an innate immune response by a genome-wide RNAi screen. *PLoS Biol* **2**, E203 (2004).
25. Kockel, L. et al. Dynamic switch of negative feedback regulation in Drosophila Akt-TOR signaling. *PLoS Genet* **6**, e1000990 (2010).
26. Mourikis, P., Lake, R.J., Firnhaber, C.B. & DeDecker, B.S. Modifiers of notch transcriptional activity identified by genome-wide RNAi. *BMC Dev Biol* **10**, 107 (2010).
27. Elwell, C.A., Ceesay, A., Kim, J.H., Kalman, D. & Engel, J.N. RNA interference screen identifies Abl kinase and PDGFR signaling in Chlamydia trachomatis entry. *PLoS Pathog* **4**, e1000021 (2008).
28. Ravi, D. et al. A network of conserved damage survival pathways revealed by a genomic RNAi screen. *PLoS Genet* **5**, e1000527 (2009).
29. Pospisilik, J.A. et al. Drosophila genome-wide obesity screen reveals hedgehog as a determinant of brown versus white adipose cell fate. *Cell* **140**, 148-160 (2010).
30. Doumanis, J., Wada, K., Kino, Y., Moore, A.W. & Nukina, N. RNAi screening in Drosophila cells identifies new modifiers of mutant huntingtin aggregation. *PLoS One* **4**, e7275 (2009).
31. Neely, G.G. et al. A genome-wide Drosophila screen for heat nociception identifies alpha2delta3 as an evolutionarily conserved pain gene. *Cell* **143**, 628-638 (2010).
32. Saj, A. et al. A combined ex vivo and in vivo RNAi screen for notch regulators in Drosophila reveals an extensive notch interaction network. *Dev Cell* **18**, 862-876 (2010).
33. Bond, D. & Foley, E. A quantitative RNAi screen for JNK modifiers identifies Pvr as a novel regulator of Drosophila immune signaling. *PLoS Pathog* **5**, e1000655 (2009).
34. Cronin, S.J. et al. Genome-wide RNAi screen identifies genes involved in intestinal pathogenic bacterial infection. *Science* **325**, 340-343 (2009).
35. Beller, M. et al. COPI complex is a regulator of lipid homeostasis. *PLoS Biol* **6**, e292 (2008).
36. Neumuller, R.A. et al. Conserved regulators of nucleolar size revealed by global phenotypic analyses. *Science signaling* **6**, ra70 (2013).
37. Korcsmaros, T. et al. Uniformly curated signaling pathways reveal tissue-specific cross-talks and support drug target discovery. *Bioinformatics* **26**, 2042-2050 (2010).
38. Kanehisa, M., Goto, S., Sato, Y., Furumichi, M. & Tanabe, M. KEGG for integration and interpretation of large-scale molecular data sets. *Nucleic Acids Res* **40**, D109-114 (2012).
39. Vinayagam, A. et al. Protein complex-based analysis framework for high-throughput data sets. *Science signaling* **6**, rs5 (2013).
40. Stark, C. et al. The BioGRID Interaction Database: 2011 update. *Nucleic Acids Res* **39**, D698-704 (2011).
41. Kerrien, S. et al. The IntAct molecular interaction database in 2012. *Nucleic Acids Res* **40**, D841-846 (2012).
42. Salwinski, L. et al. The Database of Interacting Proteins: 2004 update. *Nucleic Acids Res* **32**, D449-451 (2004).
43. Licata, L. et al. MINT, the molecular interaction database: 2012 update. *Nucleic Acids Res* **40**, D857-861 (2012).
44. Murali, T. et al. DroID 2011: a comprehensive, integrated resource for protein, transcription factor, RNA and gene interactions for Drosophila. *Nucleic Acids Res* **39**, D736-743 (2011).
45. Guruharsha, K.G. et al. A protein complex network of Drosophila melanogaster. *Cell* **147**, 690-703 (2011).

Nature Methods: doi:10.1038/nmeth.2733

46. Boyle, E.I. et al. GO::TermFinder--open source software for accessing Gene Ontology information and finding significantly enriched Gene Ontology terms associated with a list of genes. *Bioinformatics* **20**, 3710-3715 (2004).
47. Wernicke, S. & Rasche, F. FANMOD: a tool for fast network motif detection. *Bioinformatics* **22**, 1152-1153 (2006).

Nature Methods: doi:10.1038/nmeth.2733